Microarray Analysis of Gene Expression in Lung Cancer Cell Lines Treated by Fractionated Irradiation

SUNG-JA AHN[1], CHAN CHOI[2], YOO-DUK CHOI[2], YOUNG-CHUL KIM[3], KYU-SIK KIM[3], IN-JAE OH[3], HEE-JUNG BAN[3], MEE-SUN YOON[1], TAEK-KEUN NAM[1], JAE-UK JEONG[1], JOO-YOUNG SONG[1] and WOONG-KI CHUNG[1]

Departments of [1]Radiation Oncology, [2]Pathology and [3]Internal Medicine, Chonnam National University Medical School, Gwangju, Republic of Korea

Abstract. *Background: To identify differentially expressed genes between parent and radioresistant lung cancer cell lines established by fractionated irradiation. Materials and Methods: Lung cancer cell lines (A549, NCI-H1650) were irradiated with several fractionation schemes. Clonogenic assays were used to identify radioresistant cell lines. We compared the gene expression profiles on a cDNA microarray. Results: Four established cell (A549-2G, A549-5G, H1650-2G and H1650-5G) were shown to be radioresistant ($p \leq 0.05$). Seventy-two genes were commonly altered in A549-G and 655 genes in H1650-G, compared to their parental cells. Genes in the wingless-type MMTV integration site family (WNT) signaling pathway were the ones most frequently altered in both A549-G and H1650-G cells. Those involved in inflammation; integrin, platelet-derived growth factor (PDGF), interleukin, transforming growth factor-beta (TGFB), epidermal growth factor receptor (EGFR) signaling, were commonly altered in radioresistant H1650 sublines. Conclusion: The major gene expression changes during irradiation are related to WNT signaling pathway.*

Radiotherapy is generally accepted and an important therapeutic modality, particularly in patients with advanced-stage non-small cell lung cancer (NSCLC). However, individual patients may show quite different patterns of response to radiotherapy. This individual variation reflects the underlying mechanisms controlling response to radiation damage, which is determined by multiple cellular events that are controlled by a large pool of genes and their interactions. Radioresistance can be induced by exposure to a small dose of fractionated ionizing radiation, resulting in increased tolerance to the cytotoxicity caused by the succeeding irradiation (1-3). A relationship has been reported between radioresistance and expression of several genes that are predictors of radiation response. Many genetic changes are associated with radioresistance of cancer, including expression of genes controlling DNA repair, apoptosis, growth factor signaling, signal transduction, the cell cycle, cell adhesion, invasion, metastasis, angiogenesis, and hypoxia (4). Although such discoveries have partially helped understand the molecular mechanisms responsible for cellular radiosensitivity, the entire process remains to be fully elucidated. Since its development, DNA microarray technology has been applied to identify the genes associated with the inherent or acquired radioresistance in carcinomas of the lung (5, 6). Global gene expression profiling of radioresistant lung cancer cell lines may help elucidate the molecular mechanisms and pathways related to radiation response.

Based on the clinical experience that traditional standard radiotherapy of 60 Gy delivered in 30 fractions of 2 Gy each resulted in only about 20% local control in patients with advanced NSCLC, we can hypothesize that poor response to radiation may be caused by radioresistance. This resistance may be due to adaptive response of tumor cells during fractionated radiation, as well as an inherently low radiosensitivity. These radioadaptive responses determine the individual's ultimate response to radiation therapy, and so it is important to understand the underlying mechanisms controlling radioadaptive responses in NSCLC.

In our study, we tried to identify the differentially expressed genes using microarray technology to analyze gene expression in radioresistant NSCLC sublines established by fractionated irradiation with the goal of identifying the primary genes associated with the tumor response to radiation.

Correspondence to: Chan Choi, Department of Pathology, Chonnam University Medical School, 160 Baeksu-ro, Dong-gu, Gwangju, 501-746, Republic of Korea. Tel: +82 0613797071, Fax: +82 0622273429, e-mail: cchoi@chonnam.ac.kr

Key Words: Non-small cell lung cancer, radioresistance, fractionated irradiation, cDNA miroarrays.

Materials and Methods

Cells and cell cultures. The human lung cancer cell lines A594 and H1650 were provided by Young Chul Kim, M.D., Lung and Esophageal Cancer Clinic, Chonnam National University Hwasun Hospital, Republic of Korea. The cell lines were maintained in RPMI 1640 with 10% fetal bovine serum at 37˚C and 5% CO_2.

Establishment of radioresistant cell lines. The method for establishing radioresistant cell lines by fractionated irradiation is shown in Figure 1, which is a modification of a previously described method (6-8). We applied two different fractionation schemes. One is a 2-Gy fractionation (A549-2G and H1650-2G) and the other is the modified fractionation (A549-5G and H1650-5G). Briefly, on day 0, cells were counted and passaged. On day 1, cells were irradiated with 2 Gy X-radiation using a linear accelerator (Clinac IX; Varian Co., Palo Alto, USA). The irradiated cells of A549 and H1650 were cultured in conditioned medium before the next passage at approximately two weeks. This challenge was repeated every two weeks until week 26, and they were designated as A549-2G and H1650-2G, respectively. A549-5G and H1650-5G were established as follows: the parental cells were irradiated with 2 Gy of X-radiation at 2-week intervals until week 6, 3 Gy at week 8, 4 Gy at week 10, and 5 Gy from week 12 until week 26.

Clonogenic assay. Cell survival after irradiation was measured by clonogenic assay. The cultures were trypsinized to generate a single-cell suspension and 5×10^3 cells were plated in each 75-mm tissue culture dish. After allowing cells to attach for one day, they were irradiated at different doses ranging from 2 Gy to 8 Gy. These cells were incubated at 37˚C for 10-16 days (five plates in each radiation dose). After fixation with formalin and staining with 0.1% crystal violet, colonies consisting of 50 or more cells were counted under a light microscope, and the surviving fraction was determined. All survival curves represent data from at least three independent experiments.

Proliferation assay. The proliferation assay was performed using EZ-Cytox enhanced cell viability assay kit (Itsbio, Seoul, Korea) according to the manufacturer's protocol. In brief, 5×10^3 cancer cells in the logarithmic phase in 500 μl of culture medium were plated into each well of 24-well plate. They were incubated at 37˚C and in 5% CO_2 for one, two, and three days respectively. Fifty microliters of the kit solution were added to each well of the plate at the indicated time of incubation, and cells were incubated for an additional 2 h in the incubator. The absorbance was measured at 460 nm with a reference wavelength at 650 nm. The percentage of viable cells was calculated in terms of the absorbance of treated cells compared with the absorbance of untreated control cells. The proliferation assays were conducted in three independent experiments.

Total RNA extraction. For cultured cell lines, total RNA samples were extracted from each lung cancer cell line using TRIzol reagent following the manufacturer's protocol (Life Technology, Rockville, MD, USA). The quantity and quality of total RNA were assessed with a Bioanalyzer 2100 (Agilent Technologies, Santa Clara, CA, USA).

Oligonucleotide microarray. We used the commercially available Human Expression BeadChips designed using Illumina Bead Array technology (Illumina, San Diego, CA, USA) containing 48,804 genes. Briefly, 50 ng of purified total RNA was reverse transcribed to generate double-stranded cDNA using oligo(dT) (9) T7 promoter primer and MMLV reverse transcriptase. Next, cRNA was synthesized using T7 RNA polymerase, which simultaneously incorporated Cy3- or Cy5-labeled CTP. During this process, the sample of each radioresistant cell line was labeled with Cy5 whereas that of each parent cell line was labeled with Cy3 as control. One-microgram aliquot of each Cy3-labeled cRNA and Cy5-labeled cRNA were combined. They were hybridized to the microarray and scanned.

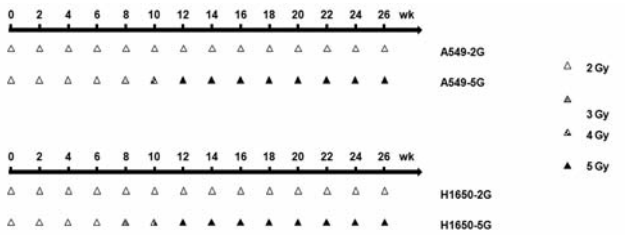

Figure 1. *Irradiation scheme to establish radioresistant lung cancer cell lines. Parental cells of A549 (A549-P) and H1650 (H1650-P) were irradiated in two ways using different fraction size and total dose of irradiation at 2-week intervals for 26 weeks. The cells harvested at the 26th week were designated as A549-2G, A549-5G, H1650-2G, H1650-5G, respectively.*

After subtraction of local and global background signals, the expression values were calculated as the log ratio of the dye-normalized red (Cy5) and green (Cy3) channel signals. Data flagged as being of poor quality by the Agilent data extraction software were removed from the analysis. All data calculated by the data extraction software were imported to the Rosetta Luminator System version 2.0 (Rosetta Biosoftware, Kirkland, WA, USA). Sequences that were 2-fold up- or down-regulated in radioresistant cells compared to parental cells were defined as being differentially regulated.

Quantitative reverse transcription PCR. Primers for the target genes were designed. The genes were bone morphogenetic protein 7 (*BMP7*); receptor tyrosine kinase-like orphan receptor 2 (*ROR2*); homolog of naked cuticle, drosophila, 2 (*NKD2*); signal transducer and activator of transcription 4 (*STAT4*); NOTCH, drosophila, homolog, drosophila, 3 (*NOTCH3*); neuronal cell adhesion molecule (*NRCAM*); mitogen-activated protein kinase 13 (*MAPK13*); matrix metalloproteinase (*MMP*) 7 (Table I). The primers for glyceraldehyde-3-phosphate dehydrogenase (*GAPDH*) were selected from Primer Bank (http://pga.mgh.harvard.edu/primerbank/ index.html).

Quantitative reverse transcription PCR (RT-PCR) was performed in Rotor-Gene™ 3000 (Corbett Research, Sydney, Australia) using Roter-Gene SYBR Green RT-PCR kit (Qiagen, Hilden, Germany). Monitoring was performed according to the manufacturer's instructions, as described previously (10). In brief, each 25-μl reaction contained 1× Rotor-Gene SYBR Green RT-PCR Master Mix, 1 μM of forward and reverse primers, Rotor-Gene RT Mix, 50 ng of template RNA, and RNase-free water. The final volume was adjusted to 5 μl with water. After the reaction mixture was loaded into the glass capillary tube, PCR was carried out under the cycling conditions according to the manufacturer's instructions. Cycling conditions were: cycle 1 (55˚C for 10 min) × 1, cycle 2 (95˚C for 5

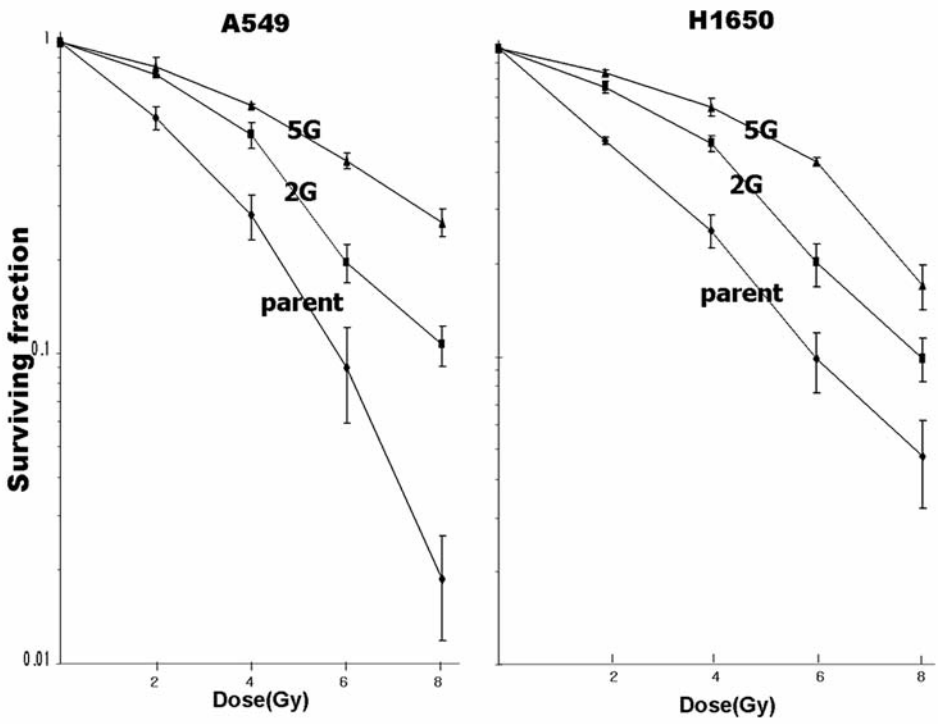

Figure 2. *Survival curves of parental cells and radioresistant cells of A549 (A) and H1650 (B). Error bars represent standards deviation from three to five independent experiments. There was a significant difference in survival fraction between parental and radioresistant cells after a single-dose radiation (0, 2, 4, 6, and 8 Gy) by ANOVA (p<0.05). Values represent the mean±SD of three to five independent experiments.*

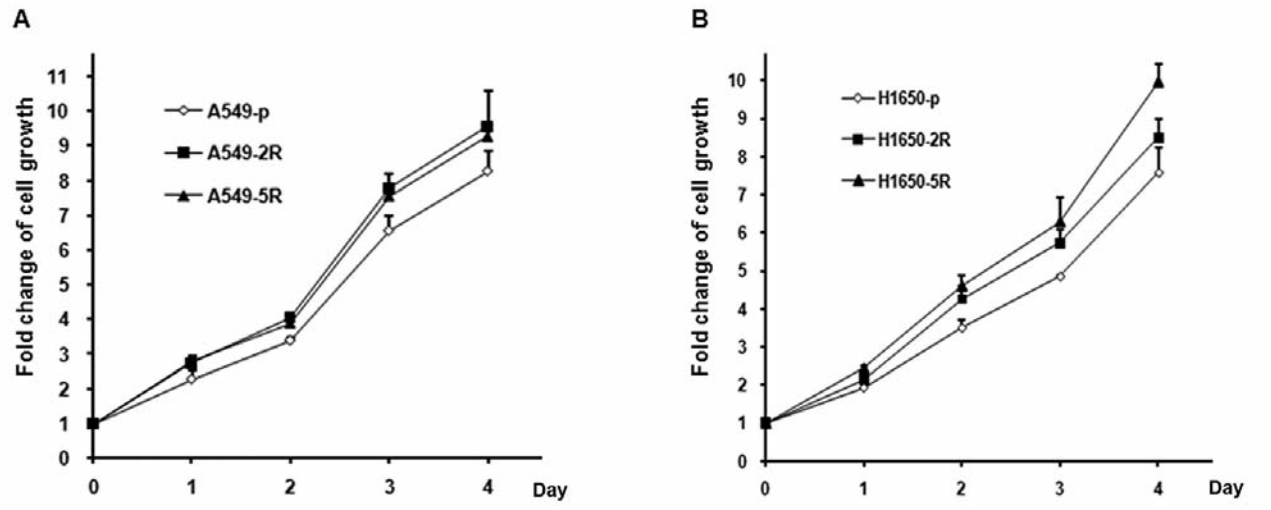

Figure 3. *Growth curve of parental and radioresistant A549 (A) and H1650 (B) cells. The effect of irradiation on cell growth was demonstrated by MTT assay at 24-h intervals until day 3. Error bars represent the SD from three independent experiments. The asterisk represents a significant difference in growth rate between parental and radioresistant cells by ANOVA (p<0.05).*

min) × 1, cycle 3 (95˚C for 5 s, 60˚C for 10 s) × 40, followed by melt curve resolution ramping from 50˚C to 99˚C increasing 1˚C every 5 seconds. Only one peak was observed for each sample. We determined expression levels of target genes and expression of *GAPDH* mRNA by comparisons with cDNA from Human Universal Reference Total RNA (Clontech, Palo Alto, CA, USA). A standard curve was produced by measuring the crossing point for each dilution of the reference standard (4-fold serially diluted cDNA of

Human Universal Reference total RNA) and plotting these crossing point values as a function of concentration on a logarithmic scale. Concentrations for each sample were calculated by plotting their crossing points against the standard curve, and these concentrations were then divided by the endogenous reference (*GAPDH*) concentration to obtain a normalized value for the expression of each gene. Each assay was performed three times to verify the results, and the mean mRNA expression was used for subsequent analysis. To investigate the biological functions involved in the discriminating genes, we utilized the PANTHER pathway database to analyze the gene expression data (11).

The specificity of the RT-PCR products was checked by agarose gel electrophoresis on 2% gels. Cycling data were examined and a cycle-threshold value was derived from the linear phase of each PCR from identical thresholds.

Statistical analysis. When comparing the surviving fractions between control and radioresistant cells in clonogenic assays and proliferation assays, repeated measurements of analysis of variance (ANOVA) method with Tukey's *post hoc* analysis were carried out. A probability level of 0.05 was chosen for statistical significance.

Results

Establishment of radioresistant cell lines. The A549 and H1650 cells were irradiated with two different fractionation schemes at 2-week intervals for 26 weeks. A549-2G and H1650-2G cells were the cell sub-lines surviving after irradiation with 2-Gy fractions for a total dose of 28 Gy. In contrast, A549-5G and H1650-5G were the cell sub-lines isolated after irradiation with fractions that ranged from 2 to 5 Gy for a total dose of 55 Gy. Surviving fractions of cells were calculated using a clonogenic assay to assess their radiosensitivity. Cell survival curves for parental cells of A549 (A549-P) and H1650 (H1650-P) and the cell sub-lines (A549-2G, A549-5G, H1650-2G, and H1650-5G) are shown in Figure 2. The surviving fraction after a dose of 2 Gy (SF2) for the parental cell line of A549 and H1650 were 0.58 and 0.4, respectively. SF2 of the A549-2G and 5G were 0.79 and 0.83 and SF2 of the H1650-2G and 5G were 0.7 and 0.8, respectively. The surviving fraction was significantly higher in the A549-2G, A549-5G, H1650-2G, and H1650-5G cell lines than that in the parental cell lines. Therefore, we considered these four cell lines (A549-2G, A549-5G, H1650-2G, and H1650-5G) to be radioresistant.

Proliferation assay. Cell growth of A549, A549-2G, and A549-5G cells was compared using the cell viability assay kit until day 3. A549-2G and A549-5G cells revealed increased proliferative activity compared an A549 cells from days 1 to 3 ($p \leq 0.05$), respectively (Figure 3A). However, no significant difference in cell growth was observed until day 3 between A549-2G and A549-5G. H1650-2G and H1650-5G had a significantly increased proliferative activity compared to H1650-P on days 2 and 3, respectively (Figure 3B). Similarly, no significant differences in cell growth were observed until day 3 between H1650-2G and H1650-5G cells.

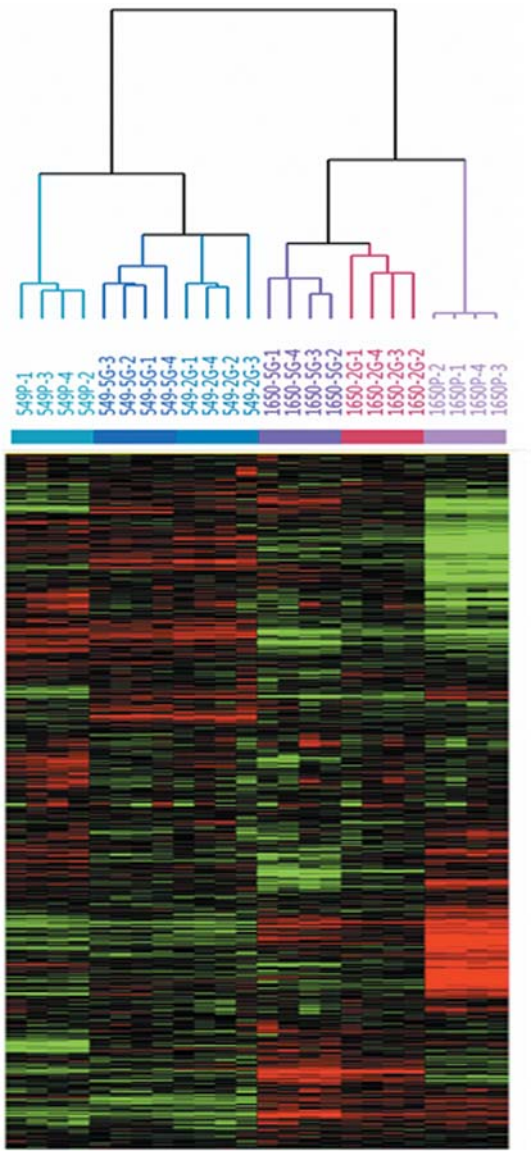

Figure 4. *Unsupervised hierarchical clustering of parental and radioresistant (2G, 5G) of A549, and H1650 cells reveals distinct genomic subgroups associated with radioresistance. Red and green colors indicate higher and lower expression, respectively, relative to the mean signal intensity of a given gene.*

Identification of differentially expressed genes. Microarray analysis revealed distinct gene expression patterns of temporal gene response to radiation for the different cell lines. We performed global expression analysis of 48,804 genes using an oligonucleotide microarray. Unsupervised hierarchical clustering showed that the radioresistant cell lines had different gene expressions compared to the parental cell lines (Figure 4). The radioresistant cell lines with lower doses of irradiation (A549-2G and H1650-2G) had different gene

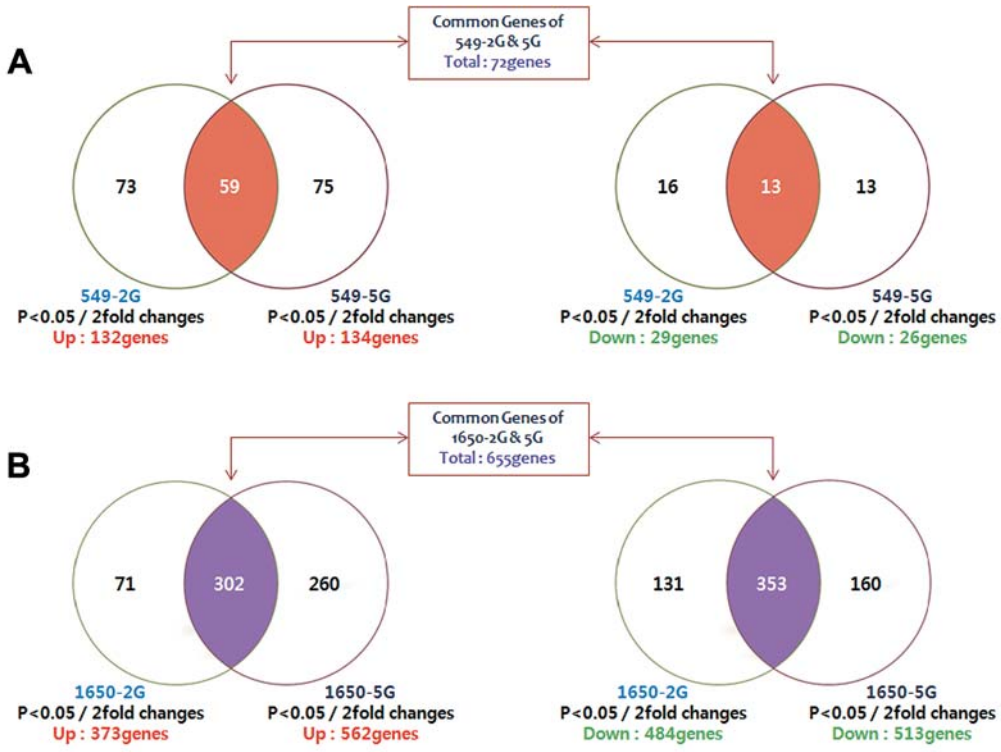

Figure 5. *Venn diagrams representing the number of transcripts differing more than two-fold in radioresistant cells compared to parental A549 (A) and H1650 (B) cells. The left diagram shows up-regulated transcripts and the right represents down-regulated transcripts.*

Table I. *Primer sequence of the genes used for quantitative reverse transcriptase polymerase chain reaction.*

Gene symbol	Amplicon length (bp)	Forward primer(5' to 3')	Reverse primer(5' to 3')
BMP7	144	ggtaattatgagcgcctacca	tcattcattcgttttattgtgacat
ROR2	143	gtacgcatggaactgtgtgacg	aaaggcaagcgatgaccagtgg
NKD2	125	ctgctcttctgccctcgat	cactccagggcctcatttt
STAT4	145	cagagccacattctccatca	ttggtgcgtcagagtttatcc
NOTCH3	140	gcctcatggcagaatagaggt	tgttaactattcctttattaggtggtg
NRCAM	113	tgccaatattttgggagaaca	ccaaatctgttgcactattacagaa
MAPK13	126	aatctgggatggaggtgttg	gcagcaataagctggggaat
MMP7	167	ggcgggaggcatgagtgagc	tgacgcgggagtttaacattccagt

BMP7, Bone morphogenic protein 7; *MAPK13*, mitogen-activated protein kinase 13; *MMP7*, matrix metalloproteinase 7; *NKD2*, naked cuticle, drosophila, homolog of, 2; *NOTCH3*, NOTCH, drosophila, homolog of, 3; *NRCAM*, neuronal cell adhesion molecule; *ROR2*, receptor tyrosine kinase-like orphan receptor 2; *STAT4*, signal transducer and activator of transcription 4.

expression patterns compared to those receiving higher doses of irradiation (A549-5G and H1650-5G). We set a cut-off of ≥2-fold for induction and ≤0.5 for repression in all experiments. Using this criterion, we identified 249 genes as differentially expressed in radioresistant A549 sub-lines: 207 genes were up-regulated and 42 genes were down-regulated. In total, 72 genes common to A549-2G and A549-5G were altered (Figure 5A). In addition, we identified 1,277 differentially expressed genes in radioresistant H1650 sub-lines: 633 genes were up-regulated and 644 genes down-regulated. A total of 655 genes common to H1650-2G and H1650-5G cells were altered (Figure 5B). The genes of the wingless-type MMTV integration site family (*WNT*) signaling pathway were the ones most frequently altered in both radioresistant A549 and H1650 cell lines. Other genes altered included those involved in inflammation mediated by

Table II. *List of genes commonly altered more than two-fold in radioresistant cells compared with parental cells according to pathway.*

Altered in H1650-2G and H1650-5G cell lines						
WNT signaling pathway						
Decreased	*GNG4*	*ITPR2*	*PCDHB17*	*SMARCA4*	*WNT5B*	
Increased	*ACTA2*	*HOXB5*	*MMP7*	*NKD2*	*PCDH9*	*SFRP4*
	TP53					
Inflammation mediated by chemokine and cytokine signaling pathway						
Decreased	*GNG4*	*ITPR2*	*RAC1*			
Increased	*ACTA2*	*CCL2*	*CCL26*	*COL5A2*	*IL6*	*PLCH1*
	PTEN	*PTGS2*	*STAT6*			
Integrin signaling pathway						
Decreased	*COL17A1*	*ITGA6*	*LAD1*	*LAMA3*	*MAP3K5*	*MAPK13*
	RAC1	*RAP1A*	*VASP*			
Increased	*COL5A1*	*COL5A2*				
PDGF signaling pathway						
Decreased	*ETS1*	*ITPR2*	*PDGFC*	*RASA1*		
Increased	*ELF3*	*PDGFRL*	*STAT4*	*STAT6*		
Interleukin signaling pathway						
Decreased	*IL1RAP*	*RASA1*				
Increased	*FOXA1*	*FOXQ1*	*IRS1*	*STAT4*	*STAT6*	
TGFB signaling pathway						
Decreased	*BMP5*	*CITED2*	*ENG*	*MAPK13*		
Increased	*BMP4*	*FOXA1*	*FOXQ1*	*GDF15*		
EGFR signaling pathway						
Decreased	*HBEGF*	*MAP3K5*	*MAPK13*	*RAC1*	*RASA1*	*TGFA*
Increased	*STAT4*	*STAT6*				
Altered in 549-2G and 549-5G cell lines						
WNT signaling pathway						
Increased	*ACTA2*	*CDH2*	*PCDHB2*	*PCDH7*		

ACTA2, Actin, alpha-2, smooth muscle, aorta; *BMP4*, bone morphogenic protein 4; *BMP5*, bone morphogenic protein 5; *CDH2*, cadherin 2; *CCL2*, chemokine CC motif, ligand 2; *CCL26*, chemokine CC motif, ligand 26; *CITED2*, CBP/p300-interacting transactivator, with Glu/Asp-rich-terminal domain, 2; *COL5A1*, collagen, type V, alpha-1; *COL5A2*, collagen, type V, alpha-2; *COL17A1*, collagen, type XVII, alpha-1; EGFR, epidermal growth factor receptor; *ENG*, endoglin; *ELF3*, E74-like factor 3; *ETS1*, v-ETS avian erythroblastosis virus E26 oncogene homolog 1; *FOXA1*, forkhead box A1; *FOXQ1*, forkhead box Q1; *GDF15*, growth/differentiation factor 15; *GNG4*, guanine nucleotide-binding protein, gamma-4; *HBEGF*, heparin-binding EGF-like growth factor; *HOXB5*, homeobox B5; *IL1RAP*, interleukin 1 receptor accessory protein; *IL6*, interleukin 6; *IRS1*, insulin receptor substrate 1; *ITGA6*, integrin, alpha-6; *ITPR2*, inositol 1,4,5-triphosphate receptor, type 2; *LAD1*, leukocyte adhesion deficiency, type 1; *LAMA3*, laminin, alpha-3; *MAP3K5*, mitogen-activated protein kinase kinase kinase 5; *MAPK13*, mitogen-activated protein kinase 13; *MMP7*, matrix metalloproteinase 7; *NKD2*, naked cuticle, drosophila, homolog of, 2; *PCDH7*, protocadherin 7; *PCDH9*, protocadherin 9; *PCDHB2*, protocadherin-beta 2; *CDHB17*, protocadherin-beta 17; *PDGF*, platelet-derived growth factor, beta polypeptide; PDGFC, platelet-derived growth factor C; *PDGFRL*, platelet-derived growth factor receptor-like; *PLCH1*, phospholipase C, eta-1; PTEN, phospholipase and tensin homolog; *PTGS2*, prostaglandin-endoperoxide synthase 2; RAC1, ras-related C3 botulinum toxin substrate 1; RAP1A, ras-related protein 1A; *RASA1*, ras p21 protein activator 1; *SFRP4*, secreted frizzled-related protein 4; *SMARCA4*, SWI/SNF-related, matrix-associated, actin-dependent regulator of chromatin, subfamily A, member 4; *STAT4*, signal transducer and activator of transcription 4; *STAT6*, signal transducer and activator of transcription 6; *TGFA*, transforming growth factor, alpha; *TGFB*, transforming growth factor, beta; *TP53*, tumor protein p53; *VASP*, vasodilator-stimulated phosphoprotein; *WNT5B*, wingless-type MMTV integration site family, member 5B.

chemokines and cytokines, integrin, platelet derived growth factor (*PDGF*), interleukin, transforming growth factor-beta (*TGFB*), epidermal growth factor receptor (*EGFR*) signaling pathway were commonly altered in radioresistant H1650 cell lines (Table II). Actin, alpha-2, smooth muscle, aorta (*ACTA2*); cadherin 2; protocadherin-beta 2; and protocadherin 7 were up-regulated in A549 sublines. *ACTA2*, protocadherin 9, and others were up-regulated in H1650 sub-lines.

A few genes were commonly up-regulated or down-regulated more than two-fold in all of the radioresistant cells compared with their parental cells. The number of up-regulated genes was 16, which include *NKD2, STAT4, NOTCH3, NRCAM*, and *MMP7*. The down-regulated genes were *BMP7, ROR2*, and *MAPK13* (Figure 6).

Validation of microarray results. To validate the expressed genes identified in microarray analyses, we performed quantitative PCR using the same RNA samples as used in the oligonucleotide microarray. We tested the expression of eight genes [*NKD2, STAT3, MMP7*, cyclin-dependent kinase inhibitor

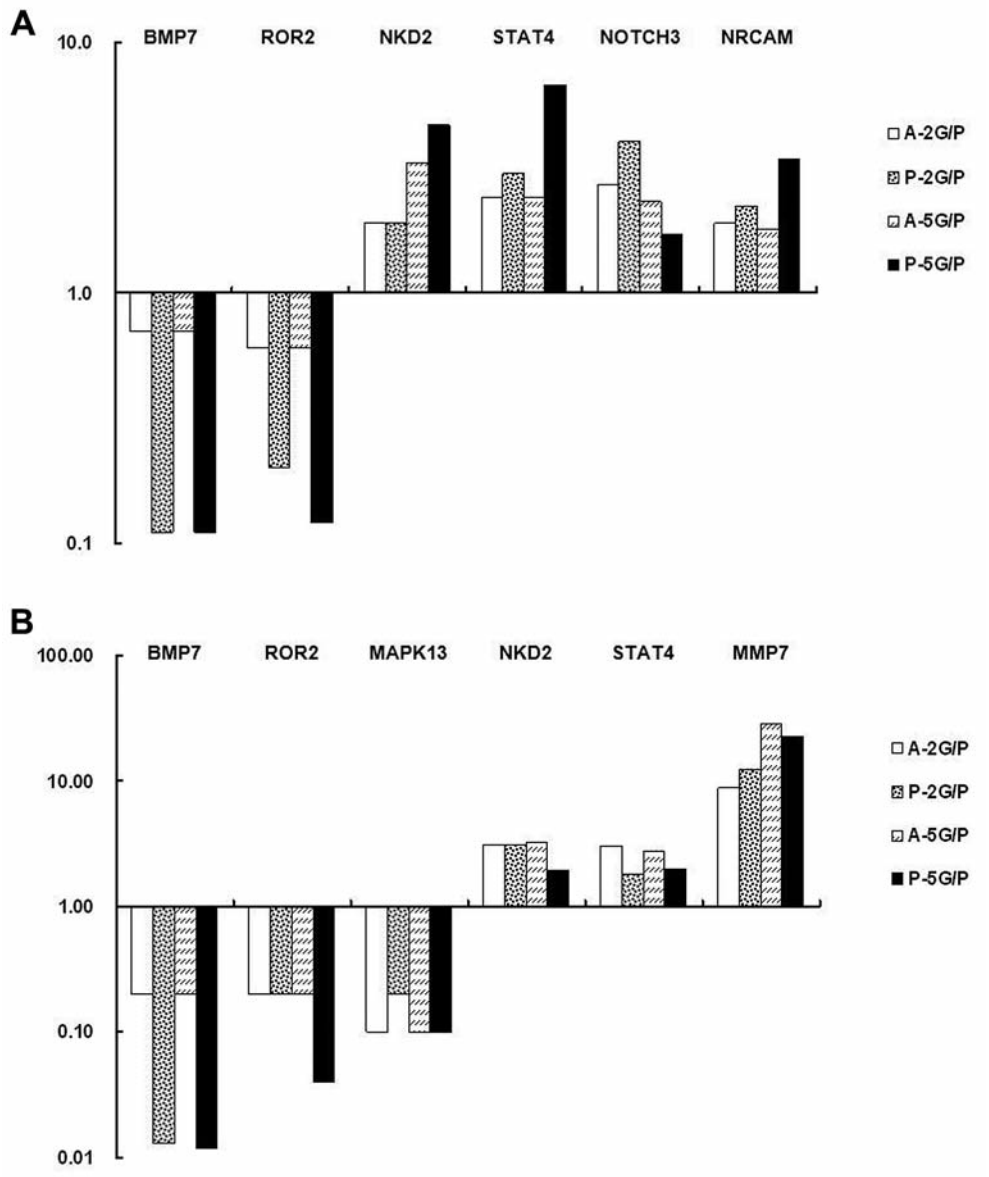

Figure 6. *Genes commonly up- or down-regulated by more than two-fold in all of the radioresistant cells compared to their parental cells are shown for A549 (A) and H1650 (B) cell lines.*

1A (*CDKN1A*), *ROR2, WNT5B, WNT5A*, and *WNT7A*] and found that the results were in good agreement with those from the microarray data, although there were some differences in the mRNA levels between A549 and H1650 cells (Figure 7).

Discussion

We examined the radiation dose-dependent and cell line-specific patterns of gene expression after irradiation using human lung cancer cell lines with different degrees of radiosensitivity. Both sub-lines exposed to higher doses of radiation were more radioresistant than those irradiated with lower doses. Radioresistant cell lines exhibited significantly higher proliferative activity than did the parental cells. However, no statistically significant difference was observed in the proliferative activity between the 2 Gy- and 5 Gy-treated resistant groups in this study. Some investigators have reported that the cell-cycle distributions are consistent in the parental and radioresistant sub-lines of lung (6) and esophageal carcinoma (12).

In the study of gene expression, the parental and radioresistant cells were differently clustered in the

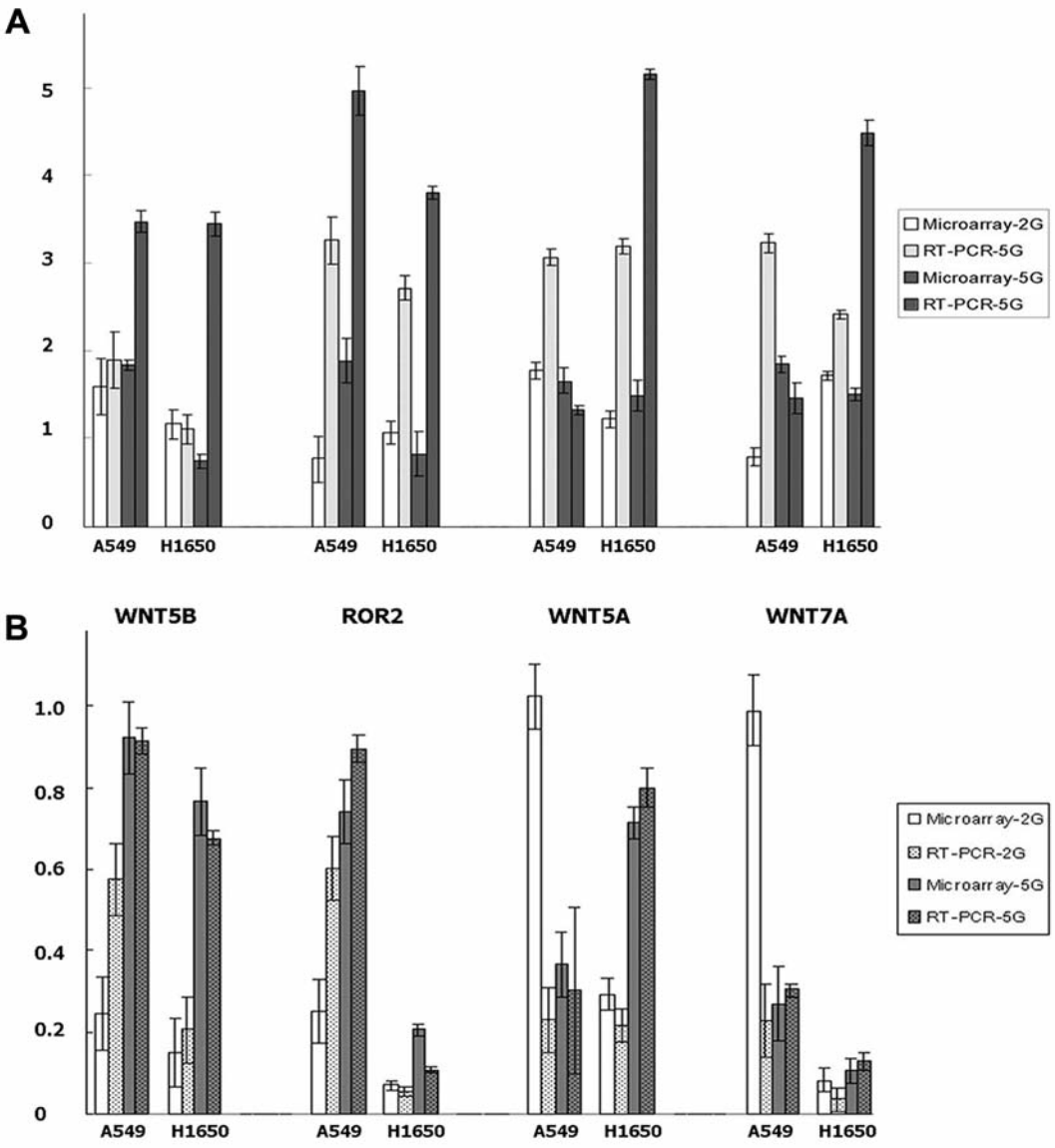

Figure 7. *Real-time quantitative PCR analysis and microarray data for selected genes up- or down-regulated in radioresistant cells compared to parental A549 (A) and H1650 (B) cells. For each gene, the first column (white) indicates the expression ratio of 2 Gy-radioresistant cells by microarray (A-2G/P), while the second column (dots) represents the expression ratio by quantitative realtime RT-PCR (P-2G/P). The third column (oblique lines) reveals the expression ratio of a 5 Gy-radioresistant cells by microarray (A-5G/P), and the fourth column (black) represents the expression ratio by quantitative realtime RT-PCR (P-5G/P). All quantitative real-time PCR data were consistent with the microarray data.*

unsupervised hierarchical clustering analysis. The number of altered genes in the parental and radioresistant sub-lines was greater for H1650 cell lines than A549 cell lines. The genes of the WNT signaling pathway were the most frequently altered both in radioresistant A549 and H1650 sublines. WNT signals are transduced through both canonical and non-canonical pathways. The canonical WNT signals are transduced through Frizzled family receptors and low-density lipoprotein receptor-related protein 5/low-density lipoprotein receptor-related protein 6 co-receptor to translocate β-catenin into the nucleus, which activates target genes. ACTA2 was commonly increased in all radioresistant sub-lines. *ACTA2* is one of six different actin isoforms. This protein is involved in cell motility, structure, and integrity. Alpha actins are a major constituent of the contractile apparatus, are a mesenchymal cell marker, and are associated with the epithelial-to-mesenchymal transition and metastasis of carcinoma (13). *ACTA2*, a marker of myofibroblast phenotype, is induced

when breast carcinoma cells are co-cultured with stromal fibroblasts (14). The genes of the cadherin superfamily are up-regulated in both of the radioresistant A549 and H1650 sub-lines. Cadherin 2 is a transmembrane molecule of the immunoglobulin superfamily, involved in neuron-neuron adhesion and directional signaling during axonal cone growth and cell-cell communication during directional cell migration. It is involved in anti-apoptosis, and its expression protects NIH3T3 cells from apoptosis by activating the extracellular signal-regulated kinase and v-akt murine thymoma viral oncogene homolog 1 signaling (15). Up-regulation of cadherin 2 mediates cohesion of breast cancer cells, and also facilitates invasion and metastasis (16). Both protocadherin-beta 2 and protocadherin 7 were up-regulated in radioresistant A549 sub-lines, and protocadherin 9 was up-regulated in radioresistant H1650 sublines. However, their functions in radioresistance or in the progression of carcinoma are still unknown. *NKD2* is one of the negative controllers of intracellular-type canonical WNT signaling pathway and acts by binding to Dishevelled (17). Up-regulation of *NKD2* should result in a constant depletion of β-catenin, which would block the control of cell adhesion and might lead to increased cell motility and invasiveness. Amplification of the *NKD2* gene due to copy number gains was observed in soft tissue malignant peripheral nerve sheath tumors (10). MMPs are zinc-dependent endopeptidases involved in tissue remodeling, proliferation, angiogenesis, apoptosis, invasion, and metastasis. They are also involved in carcinogenesis and epithelial–mesenchymal transition. The up-regulation of *MMP7* by *Helicobacter pylori* infection of stomach epithelium contributes to the development of adenocarcinoma through epithelial-mesenchymal transition (18).

STATs are a family of transcription factors regulating cell growth and differentiation. Aberrant activation of STAT signaling gives rise to cell transformation and oncogenesis. STATs play a role in tumorigenesis by means of de-regulation of the signal pathways in which they are implicated (19). Genetic variants of *STAT4* have been associated with risk of hepatitis B-virus-related hepatocellular carcinoma (20). However, the role of *STAT4* in carcinogenesis is not clearly understood yet.

NOTCH signaling is a key pathway for maintenance of stem or progenitor cells. Amplification and overexpression of *NOTCH3* has been found in NSCLC. Its target is the mitotic apparatus organizing protein discs, large (*Drosophila*) homolog-associated protein 5, which regulates the cell cycle at the G_2-M phase. Activation of the NOTCH pathway has been observed after radiation in breast cancer-initiating cells, suggesting that it is related to radiation resistance (21). Inhibition of the *NOTCH3* pathway induced apoptosis and suppressed tumor proliferation of NSCLC (22). Inhibition of the NOTCH pathway after radiation enhanced antitumor effect of radiation in NOTCH-expressing lung cancer through MAPK signaling and B-cell CLL/lymphoma 2 family proteins (23).

Recently, there is increased interest in the involvement of cancer stem cells (CSC) in radioresistance. CSCs have been found to be the main source of treatment failure after conventional fractionated radiotherapy (24). Irradiation enriches the CSC fraction and, for example, radioresistant esophageal cancer cells selected through fractionated irradiation from parental esophageal cancer cells had higher colony forming ability, proliferation, and xenograft tumorigenecity *in vivo* than their parental cells (8). WNT, NOTCH, Hedgehog and BMP signaling pathways are known to constitute the stem cell signaling network, which regulates the balance of self-renewal, proliferation, and differentiation among stem and progenitor cell populations (25). The WNT pathway has a critical role in maintenance of stem cell pluripotency. In our study, WNT signaling is one of the representative pathways associated with adaptive radioresistance. Activation of the WNT signaling pathway is a key radioprotective mechanism in irradiated cancer cells. The core proteins of the WNT pathway are β-catenin and E-cadherin. β–catenin is an essential component of both intracellular junctions and the canonical WNT signaling pathway, and has been implicated in stem cell survival (26). CSCs were found in lung cancer cell lines, and the expression of several CSC-related markers already has been confirmed in NSCLC. CSC-related markers may have utility as prognostic indicators in patients with NSCLC treated with induction chemoradiotherapy. The expression of CSC-related markers was studied using immunohistochemical staining of surgically resected specimens after chemoradiotherapy, which was significantly correlated with a poor prognosis in these patients (27).

Throughout the current study, we have observed that changes in gene expression profiles during the irradiation are related to elements of many signaling pathways, including WNT, inflammation mediated by chemokines and cytokines, integrin, PDGF, TGFB, interleukin, and the EGFR. These are likely to contribute to the complexity of radioresistance seen in NSCLC. Although the results of the study were obtained using the radioresistant cell lines established *in vitro*, these results could help elucidate the mechanism of radioresistance *in vivo*. Validation of the genes identified here could lead to new therapeutic targets for lung cancer. In further studies, the novel genes identified have to be evaluated functionally in cancer models both *in vitro* and *in vivo* to verify their association with adaptive radioresistance.

Acknowledgements

This study was supported by a grant (2007-CURIMS-DR003) of the Chonnam University Research Institute of Medical Sciences.

References

1 Shimizu T, Kato T, Tachibana A and Sasaki MS: Coordinated regulation of Radioadaptive response by protein kinase. Exp Cell Res *251*: 424-432, 1999.

2 Sasaki M, Ejima Y, Tachibana A, Yamada T, Ishizaki K, Shimizu T and Nomura T: DNA damage response pathway in radioadaptive response Mutat Res *504*: 101-118, 2002.

3 Matsumoto H, Takahashi A and Ohnishi T: Nitric oxide radicals chorepgraph a radioadaptive response. Cancer Res *67*: 8574-8579, 2007.

4 Ogawa, K, Murayama S and Mori M: Predicting the tumor response to radiotherapy using microarray analysis (Review). Oncol Rep *18*: 1243-1248, 2007.

5 Guo WF, Lin RX, Huang J, Zhou Z, Yang J, Guo GZ and Wang SQ: Identification of differentially expressed genes contributing to radioresistance in lung cancer cells using microarray analysis. Radiat Res *164*: 27-35, 2005.

6 Xu QY, Gao Y, Liu Y, Yang WZ and Xu XY: Identification of differential gene expression profiles of radioresistant lung cancer cell line established by fractionated ionizing radiation *in vitro*. Chin Med J *121*: 1830-1837, 2008.

7 Matsuyama A, Inoue H, Shibuta K, Tanaka Y, Barnard GF, Sugimachi K and Mori M: Hepatoma-derived growth factor is associated with reduced sensitivity to irradiation in esophageal cancer. Cancer Res *61*: 5714-5717, 2001.

8 Che SM, Zhang XZ, Liu XL, Chen X and Hou L: The radiosensitization effect of NS398 on esophageal cancer stem cell-like radioresistant cells. Dis Esophagus *24*: 265-273, 2011.

9 Wissmann C, Wild PJ, Kaiser S, Roepcke S, Stoehr R, Woenckhaus M, Kristiansen G, Hsieh JC, Hofstaedter F, Hartmann A, Knuechel R, Rosenthal A and Pilarsky C: WIF1, a component of the WNT pathway, is down-regulated in prostate, breast, lung, and bladder cancer. J Pathol *201*: 204-212, 2003.

10 Adamowicz M, Radlwimmer B, Rieker RJ, Mertens D, Schwarzbach M, Schraml P, Benner A, Lichter P, Mechtersheimer G and Joos S: Frequent amplifications and abundant expression of *TRIO*, *NKD2*, and *IRX2* in soft tissue sarcomas. Genes Chromosomes Cancer *45*: 829-838, 2006.

11 Mi H and Thomas P: PANTHER pathway: an ontology-based pathway database coupled with data analysis tools. Methods Mol Biol *563*: 123-140, 2009.

12 Fukuda K, Sakakura C, Miyagawa K, Kuriu Y, Kin S, Nakase Y, Hagiwara A, Mitsufuji S, Okazaki Y, Hayashizaki Y and Yamagishi H: Differential gene expression profiles of radioresistant oesophageal cancer cell lines established by continuous fractionated irradiation. Br J Cancer *91*: 1543-1550, 2004.

13 Han M, Wang Y, Liu M, Bi X, Bao J, Zeng N, Zhu Z, Mo Z, Wu C and Chen X: MiR-21 regulates epithelial-mesenchymal transition phenotype and hypoxia-inducible factor-1alpha expression in third-sphere forming breast cancer stem cell-like cells. Cancer Sci *103*: 1058-1064, 2012.

14 Buess M, Nuyten DS, Hastie T, Nielsen T, Pesich R and Brown PO: Characterization of heterotypic interaction effects *in vitro* to deconvolute global gene expression profiles in cancer. Genome Biol *8*: R191, 2007.

15 Conacci-Sorrell M, Kaplan A, Raveh S, Gavert N, Sakurai T and Ben-Ze'ev A: The shed ectodomain of Nr-CAM stimulates cell proliferation and motility, and confers cell transformation. Cancer Res *65*: 11605-11612, 2005.

16 Hazan RB, Kang L, Whooley BP and Borgen PI: N-cadherin promotes adhesion between invasive breast cancer cells and the stroma. Cell Adhes Commun *4*: 399-411, 1997.

17 Zeng W, Wharton KA Jr., Mack JA, Wang K, Gadbaw M, Suyama K, Klein PS and Scott MP: Naked cuticle encodes an inducible antagonist of Wnt signalling. Nature *403*: 789-795, 2000.

18 Yin Y, Grabowska AM, Clarke PA, Whelband E, Robinson K, Argent RH, Tobias A, Kumari R, Atherton JC and Watson SA: *Helicobacter pylori* potentiates epithelial:mesenchymal transition in gastric cancer: links to soluble HB-EGF, gastrin and matrix metalloproteinase-7. Gut *59*: 1037-1045, 2010.

19 Calò V, Migliavacca M, Bazan V, Macaluso M, Buscemi M, Gebbia N and Russo A: STAT proteins: from normal control of cellular events to tumorigenesis. J Cell Physiol *197*: 157-168, 2003.

20 Jiang DK, Sun J, Cao G, Liu Y, Lin D, Gao YZ, Ren WH, Long XD, Zhang H, Ma XP, Wang Z, Jiang W, Chen TY, Gao Y, Sun LD, Long JR, Huang HX, Wang D, Yu H, Zhang P, Tang LS, Peng B, Cai H, Liu TT, Zhou P, Liu F, Lin X, Tao S, Wan B, Sai-Yin HX, Qin LX, Yin J, Liu L, Wu C, Pei Y, Zhou YF, Zhai Y, Lu PX, Tan A, Zuo XB, Fan J, Chang J, Gu X, Wang NJ, Li Y, Liu YK, Zhai K, Zhang H, Hu Z, Liu J, Yi Q, Xiang Y, Shi R, Ding Q, Zheng W, Shu XO, Mo Z, Shugart YY, Zhang XJ, Zhou G, Shen H, Zheng SL, Xu J and Yu L: Genetic variants in STAT4 and HLA-DQ genes confer risk of hepatitis B virus-related hepatocellular carcinoma. Nat Genet *45*: 72-75, 2013.

21 Phillips TM, McBride WH and Pajonk F: The response of CD24(−/low)/CD44+ breast cancer-initiating cells to radiation. J Natl Cancer Inst *98*: 1777-1785, 2006.

22 Haruki N, Kawaguchi KS, Eichenberger S, Massion PP, Olson S, Gonzalez A, Carbone DP and Dang TP: Dominant-negative NOTCH3 receptor inhibits mitogen-activated protein kinase pathway and the growth of human lung cancers. Cancer Res *65*: 3555-3561, 2005.

23 Mizugaki H, Sakakibara-Konishi J, Ikezawa Y, Kikuchi J, Kikuchi E, Oizumi S, Dang TP and Nishimura M: γ-Secretase inhibitor enhances antitumour effect of radiation in Notch-expressing lung cancer. Br J Cancer *106*: 1953-1959, 2012.

24 Nguyen GH, Murph MM and Chang JY: Cancer stem cell radioresistance and enrichment: Where frontline radiation therapy may fail in lung and esophageal cancers. Cancers *3*: 1232-1252, 2011.

25 Pardal R, Clarke MF and Morrison SJ: Applying the principles of stem-cell biology to cancer. Nat Rev Cancer *3*: 895-902, 2003.

26 Polakis P: The many ways of Wnt in cancer. Curr Opin Genet Dev *17*: 45-51, 2007.

27 Shien K, Toyooka S, Ichimura K, Soh J, Furukawa M, Maki Y, Muraoka T, Tanaka N, Ueno T, Asano H, Tsukuda K, Yamane M, Oto T, Kiura K and Miyoshi S: Prognostic impact of cancer stem cell-related markers in non-small cell lung cancer patients treated with induction chemoradiotherapy. Lung Cancer *77*: 162-167, 2012.

Received May 4, 2014
Revised June 20, 2014
Accepted June 24, 2014